Catal Lett (2008) 122:84–90
DOI 10.1007/s10562-007-9346-8

Highly Dispersed Molybdenum Oxide Supported on HZSM-5 for Methane Dehydroaromatization

Changyong Sun · Songdong Yao · Wenjie Shen · Liwu Lin

Received: 19 October 2007 / Accepted: 2 November 2007 / Published online: 4 December 2007

Abstract Mo/HZSM-5 catalyst with highly dispersed MoO_x species was prepared by adding ammonia solution to the ammonium heptamolybdate aqueous solution during the impregnation process. Compared with the large $Mo_7O_{24}^{6-}$ species which is predominantly presented in the conventional impregnation solution, the monomer MoO_4^{2-} formed in ammonia solution could efficiently diffuse into the micropores and/or channels of the HZSM-5, resulting in higher dispersion of Mo species as well as enhanced interaction with the surface –OH groups of HZSM-5. Consequently, the obtained Mo/HSZM-5 catalyst showed rather high catalytic stability and greatly enhanced selectivity towards benzene for methane dehydroaromatization reaction by effectively inhibiting the coke formation.

Keywords Mo/HZSM-5 · Ammonia solution · Methane · Dehydroaromatization · Stability

1 Introduction

Methane dehydroaromatization to aromatics and hydrogen (MDA) is of great scientific importance and also of industrial interest for the direct conversion of natural gas [1–3]. Mo/HZSM-5 is regarded as the most active catalyst for the MDA reaction, over which near equilibrium conversion of methane could be achieved with high selectivity to benzene at 973 K [3]. It is generally accepted that the Mo/HZSM-5 catalyst is a bifunctional system, where the Mo_2C or MoO_xC_y species, formed by the reaction of MoO_x with methane during the induction period, are responsible for the activation of CH_4 and the formation of the initial C_2 species, and the Brönsted acidic sites of the HZSM-5 catalyze the oligomerization of the C_2 species to aromatics [3–6]. However, it was also observed that the methane conversion decreased drastically during the course of reaction due to the heavy coke formation, which is closely related to the strong acidic character of the HZSM-5 [2, 3, 6]. Therefore, great efforts have been paid to improve the stability of the Mo/HZSM-5 catalyst, mainly by modifying the acidic properties and the porous structures of the HZSM-5 through steaming dealumination [7, 8], external surface silanation [9–11], and hydrothermal post-synthesis [12, 13].

On the other hand, the dispersion of MoO_x on HZSM-5 is rarely concerned, although it is also an essential parameter influencing the catalytic performance of the Mo/HZSM-5 catalyst. Since wet impregnation of ammonium heptamolybdate (AHM) aqueous solution on HZSM-5 is frequently used to prepare the Mo/HZSM-5 catalyst, the interaction of Mo precursor with HZSM-5 would significantly affect the dispersion of MoO_x species in the final catalyst. Usually, large anions like $Mo_7O_{24}^{6-}$ or $H_2Mo_7O_{24}^{4-}$ are present in AHM aqueous solution at low pH value, whereas small monomer (MoO_4^{2-}) can be formed only at high pH value [14, 15]. For the typical impregnation route to prepare the Mo/HZSM-5 catalyst with pH value of 2–3, the large $Mo_7O_{24}^{6-}$ or $H_2Mo_7O_{24}^{4-}$

C. Sun · S. Yao · W. Shen (✉) · L. Lin
State Key Laboratory of Catalysis, Dalian Institute of Chemical Physics, Chinese Academy of Sciences, Dalian 116023, China
e-mail: shen98@dicp.ac.cn

L. Lin
e-mail: linliwu@dicp.ac.cn

C. Sun
Chemistry Department, Shantou University, Shantou 515063, China

anions are the main species in the AHM solution. Obviously, these large anions cannot diffuse into the micropores and/or channels of HZSM-5, and only the sequent calcination at high temperatures (>773 K) could cause the diffusion of MoO_x species into the channels of HZSM-5. By considering the fact that the rather small MoO_4^{2-} species which only presented in basic solution could easily diffuse into the micropores of HZSM-5 and further interact with the surface –OH groups, it can be expected that higher dispersion of MoO_x on HZSM-5 might be achieved in the final catalyst by impregnation in AHM ammonia solution. In fact, Datta et al. [14] revealed that higher dispersion of Mo species on SiO_2 was obtained when impregnated with ammonia solution of Mo salt than that in acidic solution. Very recently, Tan et al. [16] compared the acidity and basicity of impregnating solution of AHM on the catalytic performance of the Mo/HZSM-5 for MDA reaction, and found that impregnation of AHM on HZSM-5 in basic resulted in remarkably enhanced activity and stability for the MDA reaction.

In this work, we report the promoting effect of ammonia solution for the dispersion of molybdenum oxide on HZSM-5. The structural features of the Mo/HZSM-5 catalyst characterized with X-ray powder diffraction, solid NMR and UV–VIS diffuse reflectance was well correlated to the catalytic performance for MDA reaction.

2 Experimental

2.1 Catalyst Preparation

A commercial HZSM-5 with Si/Al mole ratio of 25 was used as support. Mo/HZSM-5-R catalyst with Mo loading of 6 wt.% was prepared by wet impregnation of ammonium heptamolybdate aqueous solution with a pH value of 2.0. After drying at 393 K overnight, the obtained solid was calcined at 773 K for 6 h in air. The Mo/HZSM-5-NH_3 (6 wt.% Mo loading) was also prepared by impregnation of ammonium heptamolybdate aqueous solution on the HZSM-5, but the pH value of the impregnation mixture was adjusted to be 9 by adding concentrated ammonia solution. The sample was then dried at 393 K overnight and finally calcined at 773 K for 6 h in air.

2.2 Characterization

Field emission scanning electron microscopy (FE-SEM) was taken on a FEI Quanta200F microscope operated at 30 kV.

Nitrogen adsorption–desorption isotherms were recorded at 77 K on a Quantachrome Autosorb-1-MP. Prior to measurement, the samples were degassed at 573 K for 6 h.

X-ray powder diffraction patterns were obtained on a Rigaku Rint D/MAX-2500/PC diffractometer using Cu Kα radiation operated at 40 kV and 100 mA.

UV–VIS diffuse reflectance spectra were collected on a Jasco V-550 UV–VIS spectrophotometer.

^{29}Si and ^{27}Al MAS NMR spectra were recorded at room temperature on a Varian Infinity-plus 400 spectrometer. Curve fitting of the ^{29}Si NMR MAS spectra was conducted using a DMFIT procedure, as previously proposed [17].

2.3 Catalytic Evaluation

Methane dehydroaromatization reaction was conducted with a continuous flow fixed-bed quartz reactor under atmospheric pressure. About 200-mg catalyst (20–40 mesh) was loaded and heated to 973 K at 10 K/min in He flow. The feed gas mixture of 90% CH_4/10% N_2 was then introduced through a mass flow controller at a flow rate of 50 mL/min. The effluent was analyzed on-line by gas chromatograph equipped with TCD and FID detectors. The conversion of methane and the selectivity of products were calculated on the basis of the mass balance of carbon using N_2 as internal standard.

The reduction and carburization of MoO_x in the Mo/HZSM-5 catalysts during the induction period of MDA reaction was investigated with a continuous flow fixed-bed reactor equipped with a mass spectrometer (Omnistar QMS200). The samples were heated to 973 K at a ramp of 10 K/min in Ar flow, and then switched to a 90%CH_4/10%He mixture, where He is used as an internal standard. Effluents from the reactor were monitored by the mass spectrometer.

3 Results and Discussion

3.1 Morphologies and Porosities

Figure 1 shows the FE-SEM images of the HZSM-5 and the Mo/HZSM-5 catalysts. The HZSM-5 mainly exhibited well-defined crystals of coffin shape with a length of 8–10 μm, a width of 4–5 μm and a thickness of 1–2 μm. Fragment aggregations less than 1 μm composed of very small individual particles were also presented. The morphologies of the Mo/HZSM-5 catalysts were almost the same as that of the HZSM-5 support, and no appreciable difference could be observed after Mo loading.

Figure 2 shows the N_2 adsorption–desorption isotherms of the HZSM-5 and the Mo/HZSM-5 catalysts.

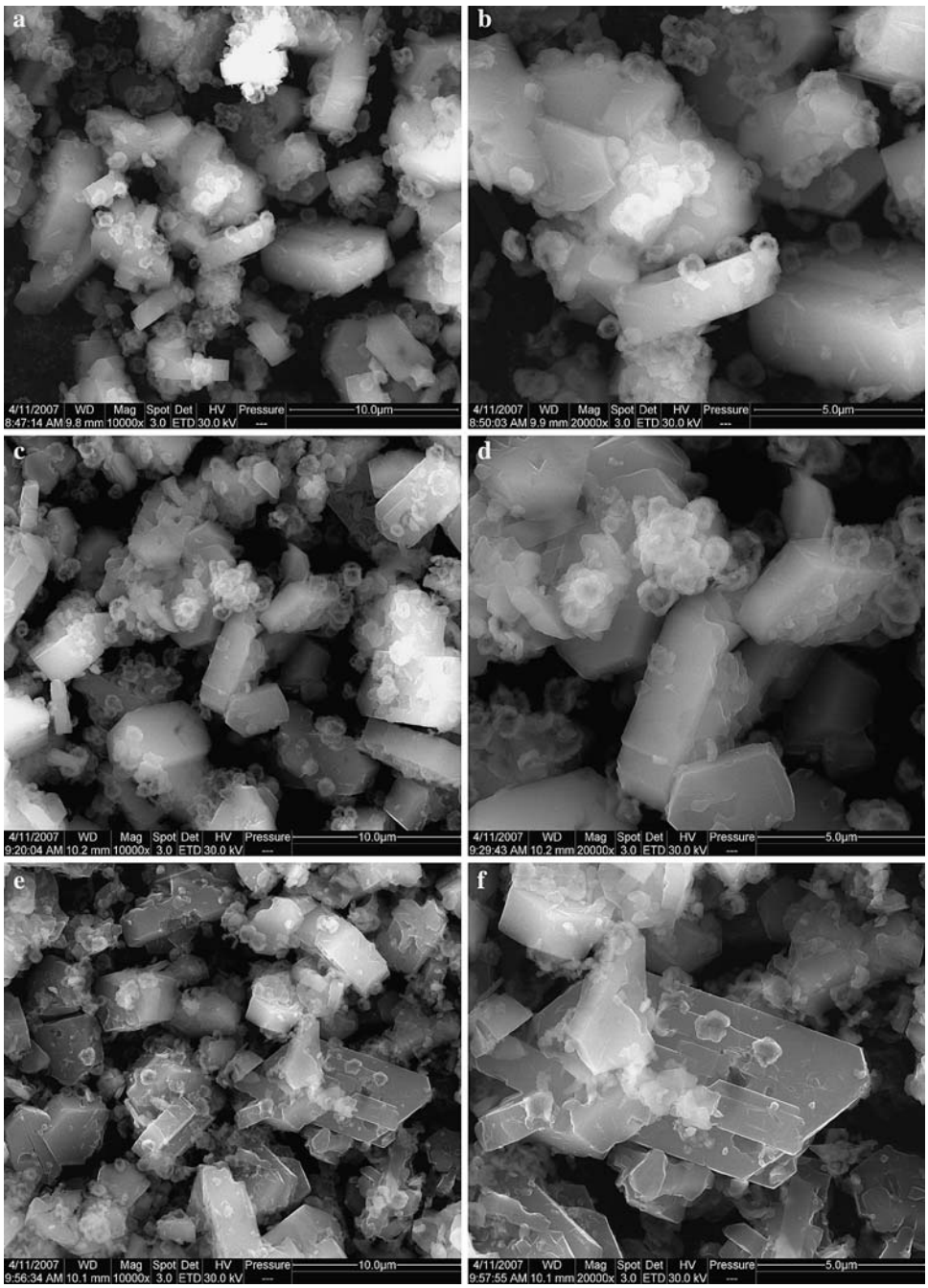

Fig. 1 FE-SEM images of HZSM-5(**a**–**b**), Mo/HZSM-5-R(**c**–**d**) and Mo/HZSM-5-NH_3(**e**–**f**)

All the samples exhibited type-I isotherm with a small identified hysteresis loop at higher p/p_0, typical for microporous materials containing a small amounts of meso- or macropores. As shown in Table 1, more than 90% of the surface area was contributed by the micropores. Mo loading decreased the surface area and the mircopore volume of the parent HZSM-5, but the Mo/HZSM-5-NH_3 catalyst still contained more micropores and less mesopores than that of the Mo/HZSM-5-R catalyst. Comparative experiments revealed that the treatment of the HZSM-5 support in ammonia solution alone decreased the mesopores, but the sequent Mo loading generated sustainable secondary pores, resulting in significantly loss of surface area and micropores. Therefore, the presence of more micropores in the Mo/HZSM-5-NH_3 catalyst could be apparently attributed to the effective interaction of the monomer MoO_4^{2-}, formed in ammonia solution, with the surface –OH groups in the micropores of the HZSM-5 during the preparation process.

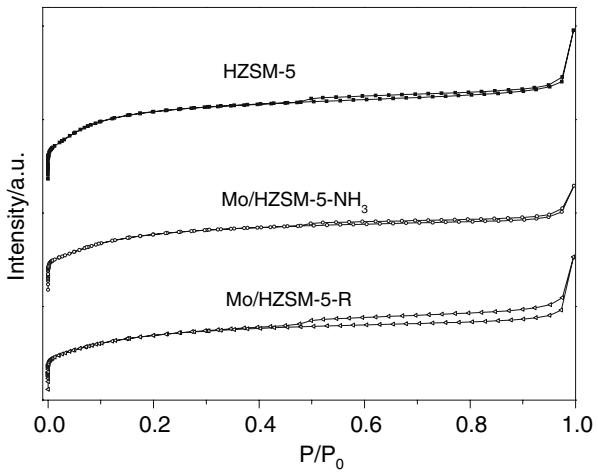

Fig. 2 N_2 adsorption–desorption isotherms of the HZSM-5 and the Mo/HZSM-5 catalysts

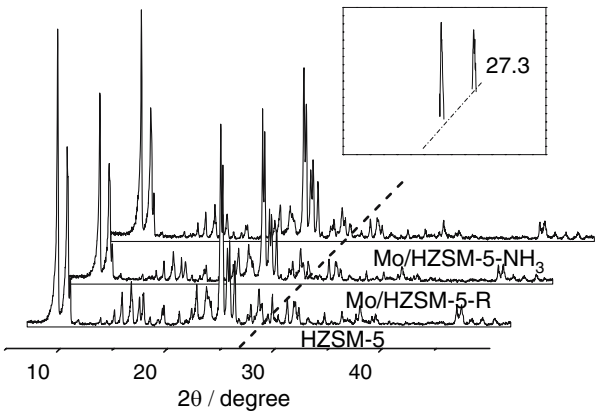

Fig. 3 XRD patterns of the HZSM-5 and the Mo/HZSM-5 catalysts. The diffractions of MoO_3 near $2\theta = 27.3°$ are shown in the inset figure

Table 1 Textural properties of the samples

Sample	S^a_{BET} ($m^2\ g^{-1}$)	S^b_{micro} ($m^2\ g^{-1}$)	V^b_{micro} ($cm^3\ g^{-1}$)	V^c_{micro} ($cm^3\ g^{-1}$)	V_{tatol} ($cm^3\ g^{-1}$)	V^d_{meso} ($cm^3\ g^{-1}$)
HZSM-5	391	361	0.149	0.161	0.227	0.083
Mo/HZSM-5-R	314	287	0.120	0.130	0.195	0.081
Mo/HZSM-5-NH_3	329	303	0.127	0.137	0.176	0.054

Calculated by [a]BET method; [b]t-plot method; [c]SF method; [d]BJH method

3.2 Dispersion of MoO_x Species

Figure 3 shows the XRD patterns of the HZSM-5 and the Mo/HZSM-5 catalysts. The typical diffraction peaks at $2\theta = 22–25°$ clearly indicated that the framework of the HZSM-5 was still retained without obvious changes of relative crystallinities after Mo loading. The weak diffractions at $2\theta = 27.3°$ verified the presence of bulk MoO_3, but the higher dispersion of molybdenum oxide in the Mo/HZSM-NH_3 catalyst than that in the Mo/HZSM-5-R sample could be clearly verified by comparing of the diffraction intensities of the MoO_3 species.

Figure 4 illustrates the UV–VIS diffuse reflectance spectra of the Mo/HZSM-5 catalysts together with a physical mixture of MoO_3 and HZSM-5. The physical mixture showed single weak characteristic absorption of Mo–O–Mo bridge bond of octahedral species at about 320 nm [18], whereas the Mo/HZSM-5 catalysts showed higher absorption intensities due to the multiple reflection effects. The absorption at 230–260 nm represented the Mo=O bond of tetrahedral molybdate and the absorption at 280 nm could be attributed to the monomer, dimer or polymerized molybdate species [18]. The phenomenon suggested that the MoO_x species with different coordination states and local symmetries were dispersed on the HZSM-5 support [19]. However, the relatively broadening absorption and slightly red shift MoO_x species in the Mo/HZSM-5-R catalyst indicated the presence of larger molybdate clusters [20]. That is, relatively small MoO_x species was formed in the Mo/HZSM-5-NH_3 catalyst than that in the Mo/HZSM-5-R catalyst, which is good accordance to the XRD observations.

Figure 5 shows the ^{27}Al and ^{29}Si MAS NMR spectra of the HZSM-5 and the Mo/HZSM-5 catalysts. The ^{27}Al spectrum of the HZSM-5 support displayed a main peak at 55 ppm and a weak peak at 0 ppm, corresponding to

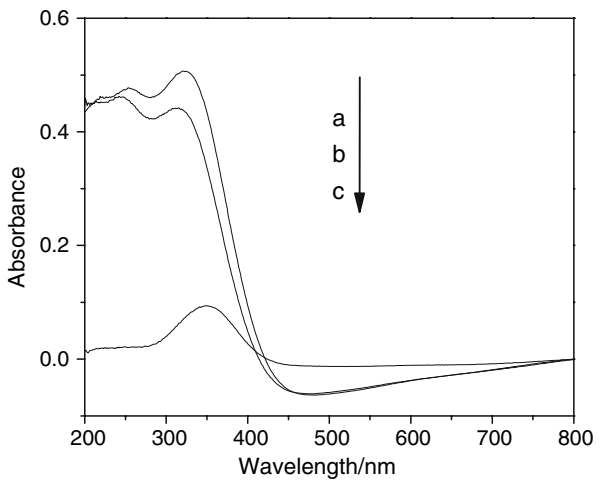

Fig. 4 UV–VIS diffuse reflectance spectra of (a) Mo/HZSM-5-R, (b) Mo/HZSM-5-NH_3 and (c) a physical mixture of MoO_3 and HZSM-5

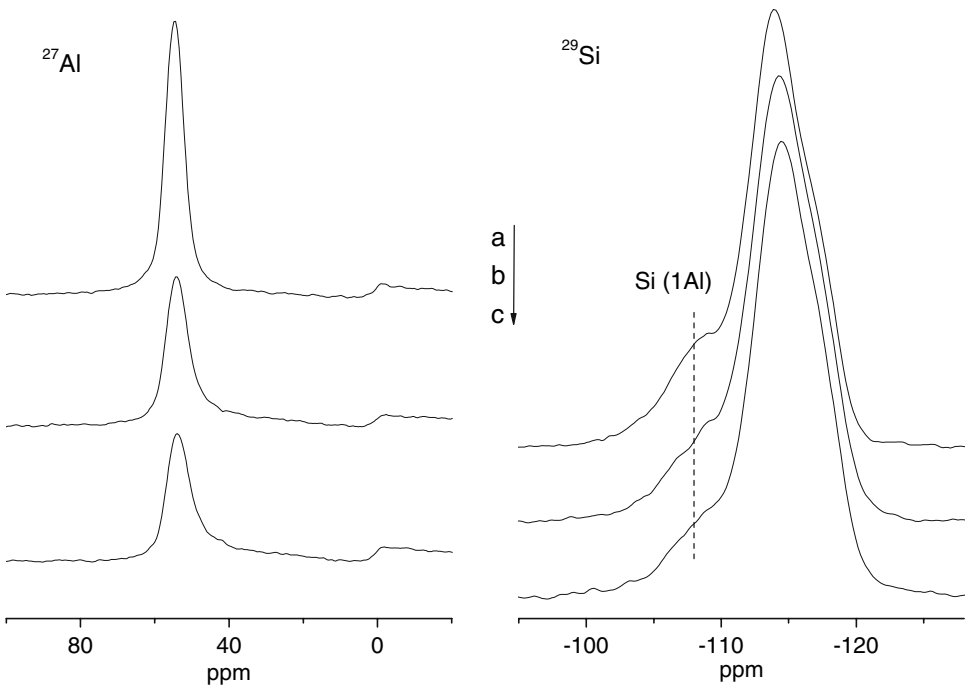

Fig. 5 ^{27}Al and ^{29}Si MAS NMR spectra of (a) HZSM-5, (b) Mo/HZSM-5-R and (c) Mo/HZSM-5- NH_3

tetrahedral Al species within zeolite frameworks and octahedral nonframework Al species, respectively [8]. Upon Mo loading, the intensities of the peak at 55 ppm dramatically decreased, but the resonance signals at 0 ppm were almost unchanged. This suggested that loading of MoO_x distorted the coordination environments of the framework Al species, and some of them might become NMR-invisible due to their lower symmetry [8]. When compared with the Mo/HZSM-5-R catalyst, the relatively lower peak of tetrahedral framework Al in the Mo/HZSM-5-NH_3 catalyst implied that more MoO_x species interacted with framework Al species. This can be further confirmed by the ^{29}Si MAS NMR spectra, which consisted of four signals at −117, −114, −108 and −103 ppm, attributed to two crystallographically inequivalent Si (0Al) sites, Si (1Al) and silanol, respectively [8]. As shown in Table 2, the apparent Si/Al ratio in the Mo/HZSM-5-NH_3 catalyst was much larger than that of the Mo/HZSM-5-R catalyst, mainly due to the abundant interaction of highly dispersed Mo species with the framework Al species.

Table 2 Framework compositions of the HZSM-5 and the Mo/HZSM-5 catalysts

Sample	Si(nAl)*	δ(ppm)	Area(%)	Si/Al ratio
HZSM-5	Si(0Al)	−117.2	20.0	23.3
	Si(0Al)	−113.8	62.1	
	Si(1Al)	−108.4	17.2	
	Silanol	−103.5	0.7	
Mo/HZSM-5-R	Si(0Al)	−117.8	15.3	29.6
	Si(0Al)	−114.2	70.6	
	Si(1Al)	−108.4	13.5	
	Silanol	−103.2	0.6	
Mo/HZSM-5-NH_3	Si(0Al)	−117.3	22.7	36.1
	Si(0Al)	−114.2	65.8	
	Si(1Al)	−108.6	11.1	
	Silanol	−103.8	0.4	

* Calculated from the deconvolution of the ^{29}Si NMR spectra [17]

3.3 MDA Reaction

Figure 6 shows the product distribution during the induction period of MDA reaction. The MoO_x species in the Mo/HZSM-5 catalysts were initially reduced by methane into Mo_2C and/or MoO_xC_y species, as conformed by the formation of carbon oxides and water, and benzene appeared only when the reduction and carburization of MoO_x approached to a steady state. The evolution of CO, CO_2 and H_2O indicated a two-stage reduction process. The initial reduction of MoO_x by methane mainly produced CO_2 and H_2O, and the subsequent reduction led to the formation of CO. Judged by the appearance of benzene in the effluent, the induction period was postponed from 570 s over the Mo/HZSM-5-R catalyst to 720 s over the Mo/HZSM-5-NH_3 catalyst. This phenomenon further convinced that higher dispersion of MoO_x in the Mo/HZSM-5-NH_3 catalyst was presented than that in the Mo/HZSM-5-R catalyst. Since the small MoO_x clusters in the Mo/HZSM-5-NH_3

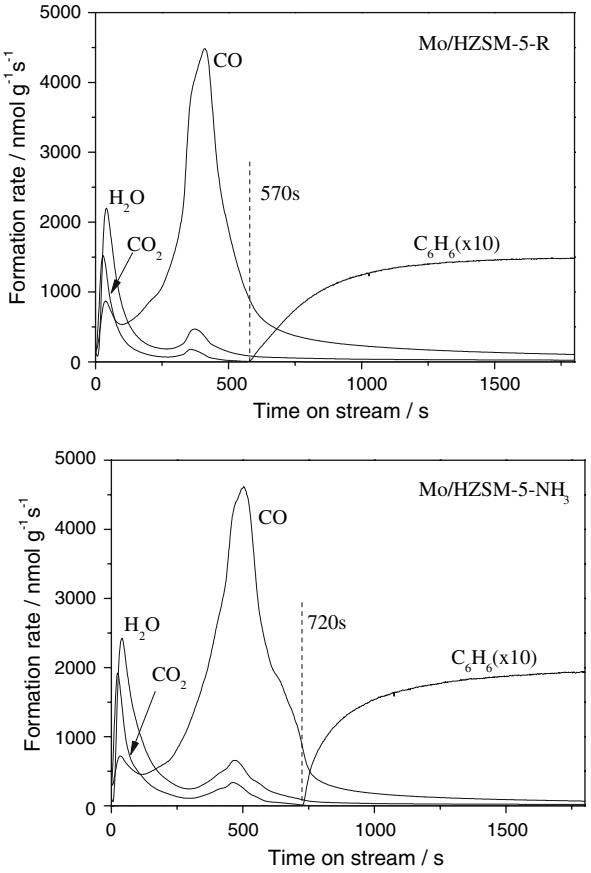

Fig. 6 Product distribution during the induction period of MDA reaction. Reaction conditions: 973 K, 0.2 g catalyst, 90% CH_4/10% He, 1,500 mL g^{-1} h^{-1}

catalyst was relatively difficult to be reduced due to the richness in the micropores and the strong interaction with framework Al species.

Figure 7 compares the catalytic performances of the Mo/HZSM-5 catalysts for MDA reaction as a function of time on stream. After running for 30 h, methane conversion was above 6%, benzene selectivity was 55% and naphthalene selectivity was 10% over the Mo/HZSM-5-NH_3 catalyst. In contrast, the methane conversion over the Mo/HZSM-5-R catalyst rapidly dropped to 3% with benzene selectivity of about 32% and naphthalene selectivity of 2.6% after running for 30 h. Moreover, heavy coke deposition was observed on the Mo/HZSM-5-R catalyst, and thus led to significant decrease in methane conversion and selectivity to benzene with time on stream. Obviously, the Mo/HZSM-5-NH_3 catalyst exhibited higher methane conversion and remarkably enhanced selectivity to benzene and naphthalene, and thus the stability was greatly improved due to the less coke deposition.

4 Conclusion

Highly dispersed MoO_x species on HZSM-5 was obtained by adding ammonia solution in the impregnating solution of Mo precursor. The monomer MoO_4^{2-} presented only at higher pH value could efficiently diffuse into the micropores and/or channels of the HZSM-5, resulting in higher dispersion of Mo species as well as enhanced interaction

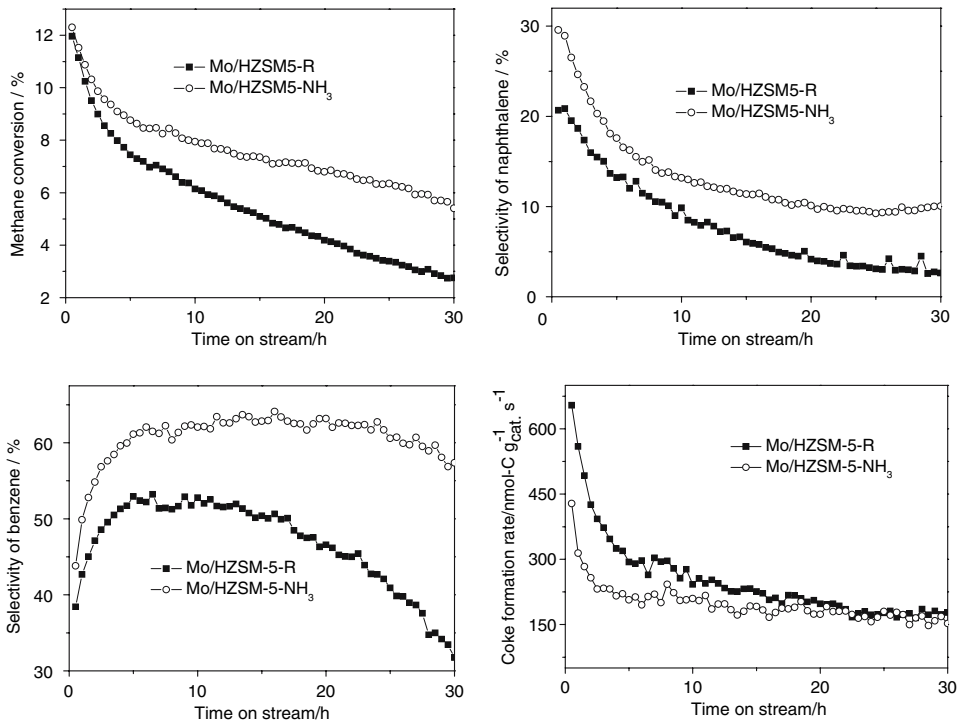

Fig. 7 Catalytic performances of the Mo/HZSM-5 catalysts for MDA reaction. Reaction conditions: 973 K, 0.2 g catalyst, 90% CH_4/10% N_2, 1,500 mL g^{-1} h^{-1}

with the surface –OH groups. Consequently, the Mo/HSZM-5 catalyst synthesized with the mediation of ammonia solution exhibited significantly improved catalytic performance for the MDA reaction in terms of methane conversion, benzene selectivity and stability.

Acknowledgment Financial support from the National Basic Research Program of China (2005CB221407) is highly appreciated.

References

1. Lunsford JH (2000) Catal Today 63:165
2. Xu Y, Lin L (1999) Appl Catal A 188:53
3. Xu Y, Bao X, Lin L (2003) J Catal 216:386
4. Ding W, Li S, Meitzner GD, Iglesia E (2001) J Phys Chem B 105:506
5. Sarioglan A, Erdem-Senatalar A, Savasci OT, Taarit YB (2004) J Catal 228:114
6. Liu H, Bao X, Xu Y (2006) J Catal 239:441
7. Lu Y, Ma D, Xu Z, Tian Z, Bao X, Lin L (2001) Chem Commun 2048
8. Ma D, Lu Y, Su L, Xu Z, Tian Z, Xu Y, Lin L, Bao X (2002) J Phys Chem B 106:8524
9. Ding W, Meitzner GD, Iglesia E (2002) J Catal 206:14
10. Liu H, Li Y, Shen W, Bao X, Xu Y (2004) Catal Today 93–95:65
11. Kikuchi S, Kojima R, Ma H, Bai J, Ichikawa M (2006) J Catal 242:349
12. Song Y, Sun C, Shen W, Lin L (2006) Catal Lett 109:21
13. Song Y, Sun C, Shen W, Lin L (2007) Appl Catal A 317:266
14. Datta AK, Ha JW, Regalbuto JR (1992) J Catal 133:55
15. Bourikas K, Hiemstra T, Van Riemsdijk WH (2001) J Phys Chem B 105:2393
16. Tan PL, Au CT, Lai SY (2007) Appl Catal A 324:36
17. Engelhardt G (1991) Solid state NMR spectroscopy applied to zeolites. In: van Bekkum H, Flanigen EM, Jansen JC (eds) Studies in surface science and catalysis. Elsevier, Amsterdam
18. Xiong G, Feng Z, Li J, Yang Q, Ying P, Xin Q, Li C (2000) J Phys Chem B 104:3581
19. Braun S, Appel LG, Camorim VL, Schmal M (2000) J Phys Chem B 104:6584
20. Fournier M, Louis C, Che M, Chaquin P, Masure D (1989) J Catal 119:400